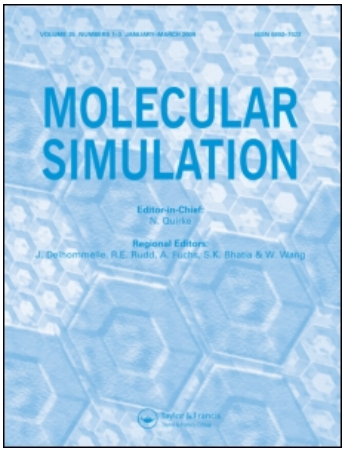

Molecular Simulation
Publication details, including instructions for authors and subscription information:
http://www.informaworld.com/smpp/title~content=t713644482

Molecular simulations of DNA transport in solution

C. M. Payne[a]; X. Zhao[b]; P. T. Cummings[b]
[a] Department of Chemical Engineering, Vanderbilt University, Nashville, TN, USA [b] Oak Ridge National Laboratory, Nanomaterials Theory Institute, Center for Nanophase Materials Sciences, Oak Ridge, TN, USA

To cite this Article Payne, C. M. , Zhao, X. and Cummings, P. T.(2007) 'Molecular simulations of DNA transport in solution', Molecular Simulation, 33: 4, 399 — 403
To link to this Article: DOI: 10.1080/08927020601154355
URL: http://dx.doi.org/10.1080/08927020601154355

Molecular Simulation, Vol. 33, Nos. 4–5, 15–30 April 2007, 399–403

Taylor & Francis
Taylor & Francis Group

Molecular simulations of DNA transport in solution

C. M. PAYNE†*, X. ZHAO‡ and P. T. CUMMINGS†‡

†Department of Chemical Engineering, Vanderbilt University, Nashville, TN 37235, USA
‡Oak Ridge National Laboratory, Nanomaterials Theory Institute, Center for Nanophase Materials Sciences, Oak Ridge, TN 37831, USA

(Received June 2006; in final form November 2006)

A proposed novel nanotechnology concept utilizes tunneling conductance measurements across nanoelectrodes to identify individual nucleotides as a DNA strand crosses its path. Such a device offers the possibility of unprecedented rapidity in the detection of DNA sequences. Preliminary simulations of this device have indicated that single-stranded (ss)-DNA sequences behave differently depending on the location of the molecule within the device. Motivated by the similarity of the comparison of the transport properties of the ss-DNA molecule in bulk solution to experimental capillary electrophoresis data, we performed molecular dynamics (MD) simulations of ss-DNA and double-stranded (ds)-DNA in free solution to directly compare electrophoretic mobility as calculated by simulation. Drift velocity at the lowest magnitude applied electric field was consistent with expected experimental data; however, at the larger applied fields necessary under timescale constraints, drift velocity appeared inconsistent with extrapolated experimental values. The simulated electrophoretic mobility values resulting from the drift velocity calculations were also smaller than experiment.

Keywords: Molecular dynamics; DNA; Electrophoresis; Genome sequencing

1. Introduction

Interest in technology capable of high-throughput, low cost genome sequencing has risen significantly since the completion of the first sequencing effort in the Human Genome Project [1]. As a result, a novel nanotechnology concept has been proposed to detect single molecules using a nanoelectrode-gated device [2–4]. Such a technology has the theoretical capability of performing genome sequencing at a rate of 1,000,000 bp/s, thusly, revolutionizing the concept of individualized medicine.

The proposed nanotechnology concept hinges on the idea that each of the four nucleotides of which DNA is comprised (adenine, cytosine, guanine and thymine) can be uniquely identified by its tunneling conductance measurement though, at the moment, this method is still being debated [5–7]. The device concept developed to take advantage of this property consists of two nanoelectrodes positioned on a nonconductive surface so that the DNA molecule will traverse through the electrodes. The gap created by the nanoelectrodes will serve as the detection gate through which tunneling conductance measurements will be made. An illustration of the general scheme of the sequencing device is shown in figure 1(a) and (b).

Within the general device concept there exist many possible configurations, all within the realm of investigation through molecular dynamics (MD) simulations. Initial simulations of a given configuration of the conceptual device have shown that DNA behaves differently in the bulk solution than it does when in proximity to the electrode gate. We will briefly discuss these initial results; however, details of these simulations are to be presented in a future publication. As a part of the investigation into the ideal configuration of the sequencing device, we have performed preliminary simulations of both single-stranded (ss) and double-stranded (ds) DNA in a bulk aqueous environment with the intention of evaluating the electrophoretic mobility. In this article, we examine the relationship between simulated electrophoretic mobility and experimental as a means of validating implemented force fields.

2. Initial transport properties

Simulation efforts began with the device being examined in its entirety. The metal nanoelectrodes were chosen to be platinum and gold set between mica surfaces containing a 16 base pair ss-DNA molecule (eight cytosines followed

*Corresponding author. Email: christina.payne@vanderbilt.edu

Molecular Simulation
ISSN 0892-7022 print/ISSN 1029-0435 online © 2007 Taylor & Francis
http://www.tandf.co.uk/journals
DOI: 10.1080/08927020601154355

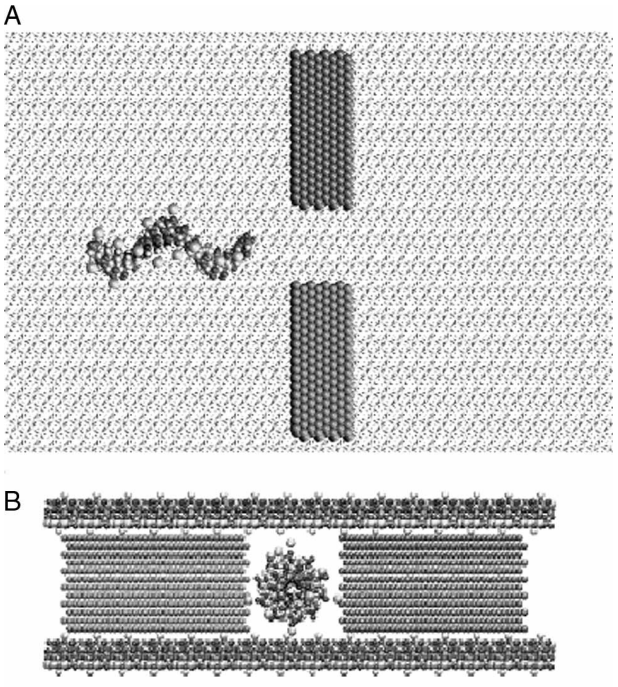

Figure 1. (A) View of the sequencing device concept pictured from above. This view does not show the top mica surface for clarity. The two electrodes, one platinum and one gold, serve as the gate through which tunneling conductance measurements will be made. (B) End view of the sequencing device showing both of the containing mica surfaces.

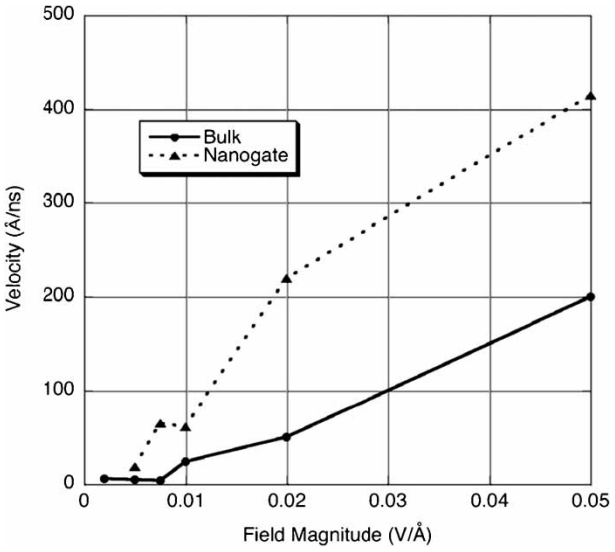

Figure 2. Plot of the velocity of the ss-DNA molecule within the sequencing device as it relates to the applied field magnitude. The position of the molecule within the device, i.e. bulk or nanogate, was determined when the molecule velocity markedly increased.

by eight thymines) and sodium counterions in water. All simulations were performed using large-scale atomic/molecular massively parallel simulator (LAMMPS) [8,9] at 300 K. After an initial equilibration period, electric fields of varying magnitudes were applied to induce motion of the ss-DNA molecule over the course of a nanosecond.

Upon applying the electric field to the system, this force became the primary contribution to DNA drift dynamics. Diffusion and conformational dynamics contributed little to the forward motion of the molecules due to the magnitudes of the applied fields except for the case of very weak applied fields. The effect of the applied electric field on the transport of the ss-DNA molecule through solution was evaluated by observing the change in position of its center of mass over the course of the simulation and thusly, its approximate velocity. Figure 2 illustrates the relationship between the velocity of the molecule and the applied electric field magnitude based on the molecule's position relative to the nanogate. Position relative to the nanogate was delineated by the marked acceleration of the molecule. The ss-DNA molecules appeared to accelerate when the first base pair was within 0.5 nm of the entrance to the gap. All molecules, with the exception of the smallest magnitude applied electric field (-0.02 V/Å), entered the device gap to some degree during the course of our simulations. This acceleration may be an artifact of the force fields used for the DNA–electrode and water–electrode interactions [10]. According to the results, the bulk velocity relationship to the electric field magnitude appeared to be nearly linear, given the rough approximation of velocity, when the field strength was stronger than -0.01 V/Å which was in agreement with previous similar simulations [11]; however, under smaller magnitude fields, the motion fell into somewhat oscillatory behavior, perhaps as a result of the short length of the simulation and possible energetic barriers to translocation. The relationship of the velocity near the nanogate to the field magnitude appeared to be nonlinear given the set of velocities available. One could compare this to what is known for nonbiological polymers translocating through nanopores, for which a consensus on the expected behavior of polymers translocating through nanopores has not been reached at this time. Over small ranges of applied fields, the drift velocity varied linearly with potentials [12]; however, over wider ranges, the relationship appeared to be more quadratic in form [13]. This could be attributed to the large number of variables involved in determining this relationship such as the pore material/polymer interactions, length of the polymer affecting velocity and energetic barriers to translocation in general.

While definitive relationships cannot be determined from this limited set of data, a comparison of the observed bulk velocities to the capillary electrophoresis mobility study performed by Stellwagen and Stellwagen [14] revealed an order of magnitude consistency in the velocity measurements. The experiment made use of a technique known as capillary zone electrophoresis, which is the electrophoretic technique that most closely approximates the bulk behavior of the simulated nanoscale device. In this experimental study, ss- and ds-DNA 20 base pair oligomers in a buffer of 40 mM Tris–acetate-EDTA at 7.6 pH were electrophoresed through a capillary coated with polyacrylamide 38.8 cm long and 100 μm in diameter at 200 V/cm (2×10^{-6} V/Å). Stellwagen noted that free

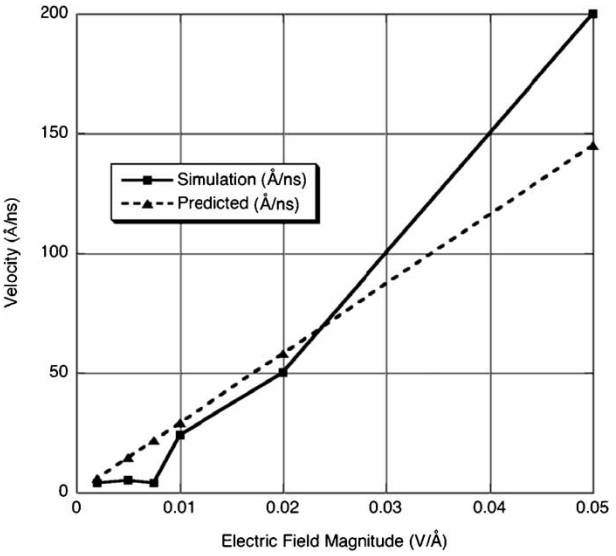

Figure 3. Relationship of bulk velocity within the sequencing device to the applied field magnitude as compared to the drift velocities predicted based on capillary electrophoresis experiments.

solution mobility of DNA increased with increasing molecular weight up to a plateau that occurred around 170 bp. A relationship between sequence and mobility was also observed in this experiment; however, for the purpose of assessing consistency between simulation and experiment, we focused on two oligomers. All sequence mobilities observed in this experiment were in the range of 2.894×10^{-4} and $2.944 \times 10^{-4}\,\mathrm{cm^2\,V^{-1}\,s^{-1}}$. With an electrophoretic field of $2 \times 10^{-6}\,\mathrm{V/Å}$, these mobilities corresponded to velocities in the range of 0.00578–0.00588 Å/ns. The experimental electrophoretic field was much smaller than the smallest magnitude field applied in the simulation of the sequencing device; therefore, figure 3 is an illustration of the predicted velocities based on an assumed linear relationship to electric field magnitude as compared to observed bulk simulation velocities. Given the slight differences in the experimental and simulated environment, the velocities observed in simulation were consistent with the predicted velocities based on experimental data.

3. Electrophoresis simulations

3.1 Simulation details

In light of the results based on the simulation of the entire sequencing device, we performed a series of simulations of both ss- and ds-DNA molecules in pure water similar to ss-RNA MD simulations performed by Yeh and Hummer [11] in order to more directly compare simulation results to experiment. The experiment authors, Stellwagen and Stellwagen electrophoresed several different configurations of ss-DNA molecules as well as several ds-DNA molecules. We chose to compare our simulations to the experimental results of Stellwagen over another ss-DNA electrophoretic mobility study by Hoagland [15] because of the smaller oligomers used in the Stellwagen study. Hoagland *et al.* studied the electrophoretic mobility of ss-DNA molecules consisting of tens of thousands of base pairs. This simulation study focused on the ss-DNA oligomer denoted ssA5, which consisted of the following sequence of nucleotides, CGCAAAAACGCGCAAA-AACG, as well as the ds-DNA oligomer denoted dsA5, which was a double strand DNA molecule consisting of the ssA5 sequence and its complement.

The MD simulations of ssA5 and dsA5 were performed using LAMMPS with the CHARMM 27 all-hydrogen force field [16,17]. Explicit water was described by the TIP3P model [18]. The sodium counterions were represented by a potential developed by Beglov and Roux [19]. Initial coordinates for the ssA5 and dsA5 molecules were generated using nucleic acid builder (NAB) [20,21]. The molecules were solvated and neutralized with sodium (Na^+) counterions using a script within the LAMMPS software package. At a density of 1 g/cc, 3802 water molecules solvated the ssA5 molecule in addition to 20 sodium counterions. The dsA5 molecule was solvated with 3486 water molecules and 40 sodium counterions.

The simulations utilized periodic boundary conditions and were equilibrated for 1 ns using the *NPT* ensemble at 300 K and 101,325 Pa with the Nosé–Hoover thermostat [22] and barostat [23]. Time integration was performed using the velocity-Verlet algorithm [24] with a timestep of 2 fs. The hydrogen bonds were constrained using the SHAKE algorithm [25]. Long-range Coulombic interactions were computed using a particle–particle–particle–mesh (PPPM) solver [26].

After the equilibration period, the simulations were restarted with the addition of an applied uniform external electric field of varying magnitudes (0.003, 0.03, 0.04 and 0.05 V/Å) and run for 1.5 ns. As in the previous simulations, these applied field magnitudes were significantly larger than those typically used in capillary electrophoresis experiments due to the timescale limitations of molecular simulation.

3.2 Results and discussion

In order to evaluate the electrophoretic mobility of the simulated DNA molecules, we first had to determine the drift velocity of the molecule. Figure 4(a) and (b) show the change in position of the ssA5 and dsA5 molecules, respectively, from their original position in the z-direction (the direction of the applied electric field). The change in position was evaluated by monitoring the center of mass of the molecule. The drift velocity for each applied field magnitude was determined from the slope of the relatively linear change in position over time. In most cases, the change in position over time increased as the applied field magnitude increased resulting in a larger drift velocity. The behaviours of the ssA5 molecule when the 0.03 and 0.04 V/Å fields were applied were the only exceptions. These two cases seemed to oscillate in roughly the same positions resulting in approximately the same drift

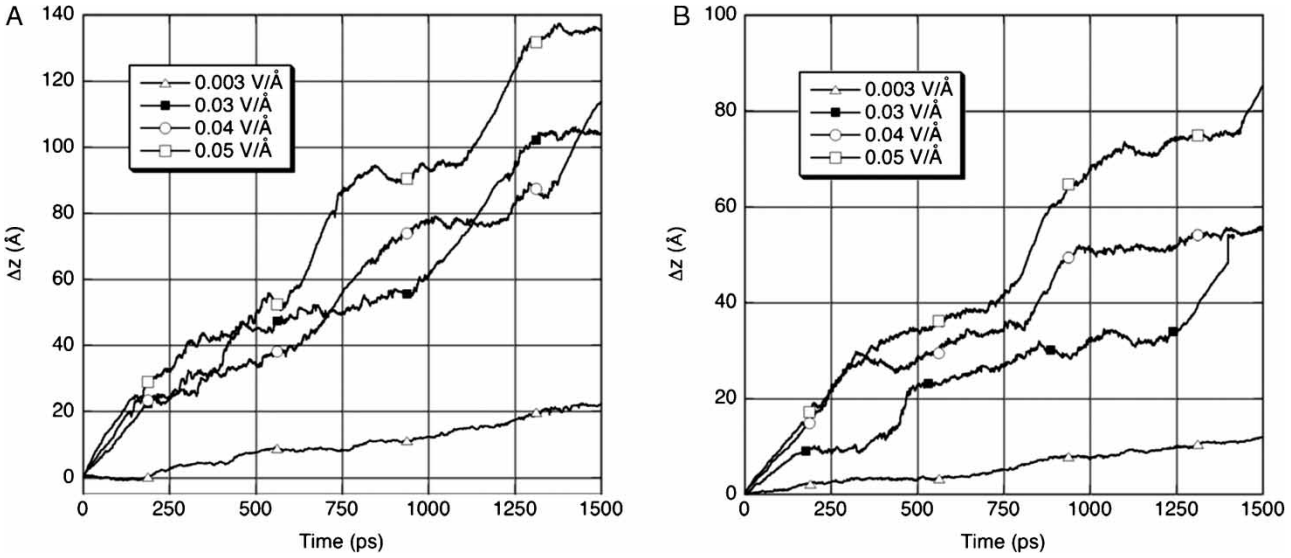

Figure 4. (A) Center of mass motion in the z-direction for the ssA5 molecule vs. time for applied fields 0.003, 0.03, 0.04 and 0.05 V/Å. (B) Center of mass motion in the z-direction for the dsA5 molecule vs. time for applied fields 0.003, 0.03, 0.04 and 0.05 V/Å. The open triangles, circles, squares and filled squares are not representative of data points but merely a method of differentiating lines.

velocities despite the varying field magnitude. We note that for the larger magnitude applied fields, there appeared to be an emergent "step pattern" in the change in position vs. time though this behaviour was not as apparent in visualizations. We conjecture that averaging $\Delta z(t)$ over many trajectories may eliminate the steps evident in the current single trajectory results reported here. This requires further study. Such behavior was not evident in electrophoresis experiments as the applied fields used experimentally were of significantly lower magnitude than those applied in simulation.

Figure 5 illustrates the correlation of the drift velocities obtained as above with the applied electric field. There is an assumed linear relationship between electric field magnitude E, and drift velocity, v, where the electrophoretic mobility, μ, is a proportionality constant, i.e. $v = \mu E$. Based on this relationship, we have extrapolated an experimental drift velocity for each of the simulated electric field magnitudes for comparison to simulated drift velocity. As one can see, the simulated drift velocities were somewhat lower than the extrapolated experimental values for the larger magnitude electric fields; however, the simulated drift velocities of both ssA5 and dsA5 for the 0.003 V/Å magnitude were consistent with experiment.

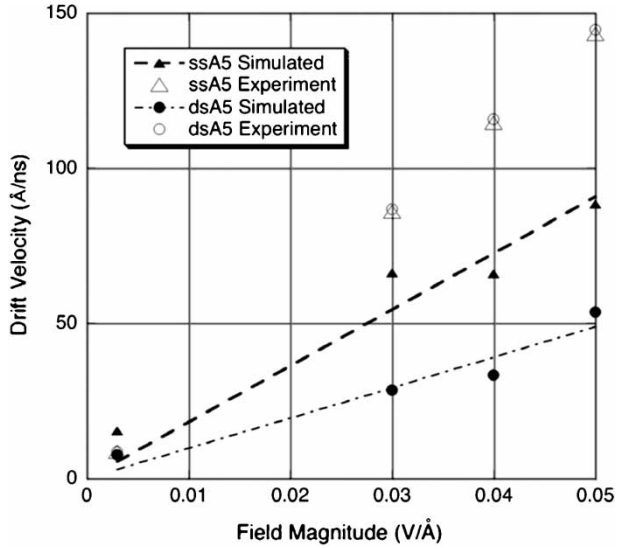

Figure 5. Drift velocity of ssA5 and dsA5 as a function of applied electric field. The dashed and dot-dashed lines are the linear fits of the ssA5 and dsA5 drift velocity vs. electric field data, respectively, through which electrophoretic mobility was determined.

The values of the simulated mobility were calculated from the slope of the linear fit to the drift velocity data. Significantly strong electric fields can result in nonlinear electrophoretic mobilities [27]; however, in experimental capillary electrophoresis and in this simulation study, the linear regime was applicable. Here, electrophoretic mobility was calculated as 1.8×10^{-4} and $9.8 \times 10^{-5}\,\mathrm{cm^2\,V^{-1}\,s^{-1}}$ for ssA5 and dsA5, respectively. Compared with the experimental values for ssA5 at 2.87×10^{-4} and dsA5 at $2.89 \times 10^{-4}\,\mathrm{cm^2\,V^{-1}\,s^{-1}}$, we can see that simulation in the above described manner resulted in a lower electrophoretic mobility (by 35% for ssA5 and by 65% for dsA5). This could result from the viscosity difference of using pure water as the solvent in simulations as opposed using the buffer used in experiments. Additionally, the simulations had no physical boundary such as the experimental capillary, which could augment mobility, though in theory, this effect was corrected for in the experiments. Of more concern was that the simulated electrophoretic mobility of the larger molecule, dsA5, was smaller than that for the ssA5 molecule, while the experimental observations indicated that the larger molecule should have a slightly larger mobility. The experimental results were counter-intuitive (i.e. the experimental result indicated that the larger molecule had slightly higher mobility) and so the

significance of the disagreement in the trends between simulation and experiment was difficult to gauge. Additionally, we note that the experimental mobilities for ss- and ds-DNA may not be statistically significantly different, once error estimates were taken into account. Though Stellwagen and Stellwagen reported no error values for the normalized mobilities, error propagation of the measured values to the normalized values used in this study indicated that the mobilities of both dsA5 and ssA5 were statistically the same.

It is interesting to note that the mobilities calculated in the bulk simulations (i.e. with no nanogate present) were lower than those found in the bulk regime of the nanogate simulation. One possibility was that the convective motion induced in the solvent by the field acting on the DNA and its counterions was enhanced in the presence of the nanogate because of the collimating effect of the nanogate, thus resulting in greater directionality of the DNA motion in the direction of the applied field. This could be tested by simulations in the presence of the nanogate in which the field is applied perpendicular to the nanogate opening.

4. Conclusions

We have performed simulations of two DNA molecules, ssA5 and dsA5, in bulk aqueous solution using classical MD simulations in order to determine electrophoretic mobilities. Results from the ssA5 and dsA5 simulations in bulk water compared to initial simulations of ss-DNA confined between two mica plates and experimental capillary electrophoresis experiments were inconsistent at larger applied electric field magnitudes. The simulated electrophoretic mobilities were notably smaller likely due to freedom of motion through periodic boundary conditions. Future work in this area will include the constraint of the DNA molecules in the *x*- and *y*-directions as well as examining lower magnitude fields over longer timescales.

Acknowledgements

We would like to thank Dr Paul Crozier for valuable discussions regarding the use of simulation codes. These simulations were performed using the ACCRE computational facilities at Vanderbilt University, Nashville, TN. Financial support from the NIH (1R21HG003578-01) and DOE CSGF fellowship support (DE-FG02-97ER25308) is gratefully acknowledged.

References

[1] J.C. Venter, M.D. Adams, et al. The sequence of the human genome. *Science*, **291**, 1304 (2001).

[2] J.W. Lee, E. Greenbaum. Programmable nanometer-scale metal bonding to single molecules by electrolytic deposition and depletion. ORNL Invention Disclosure ID 0772 (1999).

[3] J. Lee, T. Thundat, et al. DNA and RNA sequencing by nanoscale reading through programmable electrophoresis and nanoelectrode-gated tunneling and dielectric detection. ORNL Invention Disclosure ID 0943. US Patent Appl. Publ., pp. 24 (2003) CODEN: USXXCO US 2003141189 A1.

[4] J.W. Lee, E. Greenbaum. Programmable nanometer-scale electrolytic metal deposition and depletion. U.P. Office 6,447,663 B1 (2002).

[5] R. Zikic, P.S. Krstic, et al. Characterization of the tunneling conductance across DNA bases. *Phys. Rev. E. Stat. Nonlin. Soft Matter Phys.*, **74**, 011919 (2006).

[6] X.G. Zhang, P.S. Krstic, et al. First-principles transversal DNA conductance deconstructed. *Biophys. J.*, **91**, L04 (2006).

[7] J. Lagerqvist, M. Zwolak, et al. Fast DNA sequencing via transverse electronic transport. *Nano Lett.*, **6**, 779 (2006).

[8] S. Plimpton. Fast parallel algorithms for short-range molecular dynamics. *J. Comput. Phys.*, **117**, 1 (1995).

[9] LAMMPS, www.cs.sandia.gov/~sjplimp/lammps.html.

[10] C.M. Payne, X. Zhao, et al. Molecular dynamics simulation of DNA translocation through a copper nanoelectrode gap (in preparation).

[11] I.-C. Yeh, G. Hummer. Diffusion and electrophoretic mobility of single-stranded RNA from molecular dynamics simulations. *Biophys. J.*, **86**, 681 (2004).

[12] J.J. Kasianowicz, E. Brandin, et al. Characterization of individual polynucleotide molecules using a membrane channel. *PNAS*, **93**, 13770 (1996).

[13] A. Meller, L. Nivon, et al. Voltage-driven DNA translocations through a nanopore. *Phys. Rev. Lett.*, **86**, 3435 (2001).

[14] E. Stellwagen, N.C. Stellwagen. Determining the electrophoretic mobility and translational diffusion coefficients of DNA molecules in free solution. *Electrophoresis*, **23**, 2794 (2002).

[15] D.A. Hoagland, E. Arvanitidou, et al. Capillary electrophoresis measurements of the free solution mobility for several model polyelectrolyte systems. *Macromolecules*, **32**, 6180 (1999).

[16] N. Foloppe, A.D. MacKerell. All-atom empirical force field for nucleic acids: I. Parameter optimization based on small molecule and condensed phase macromolecular target data. *J. Comput. Chem.*, **21**, 86 (2000).

[17] A.D. MacKerell, N.K. Banavali. All-atom empirical force field for nucleic acids: II. Application to molecular dynamics simulations of DNA and RNA in solution. *J. Comput. Chem.*, **21**, 105 (2000).

[18] W.L. Jorgensen, J. Chandrasekhar, et al. Comparison of simple potential functions for simulating liquid water. *J. Chem. Phys.*, **79**, 926 (1983).

[19] D. Beglov, B. Roux. Finite representation of an infinite bulk system: solvent boundary potential for computer simulations. *J. Chem. Phys.*, **100**, 9050 (1994).

[20] T. Macke, D.A. Case. *Modeling Unusual Nucleic Acid Structures*, American Chemical Society, Washington, DC (1998).

[21] The NAB molecular manipulation language, http://www.scripps.edu/mb/case/

[22] H.J.C. Berendsen, J.P.M. Postma, et al. Molecular dynamics with coupling to an external bath. *J. Chem. Phys.*, **81**, 3684 (1984).

[23] G.J. Martyna, D.J. Tobias, et al. Constant pressure molecular dynamics algorithms. *J. Chem. Phys.*, **101**, 4177 (1994).

[24] M.P. Allen, D.J. Tildesley. *Computer Simulations of Liquids*, Clarendon Press, Oxford (1987).

[25] J.-P. Ryckaert, G. Ciccotti, et al. Numerical integration of the Cartesian equations of motion of a system with constraints: molecular dynamics of *n*-alkanes. *J. Comput. Phys.*, **23**, 327 (1977).

[26] R.W. Hockney, J.W. Eastwood. *Computer Simulation Using Particles*, A. Hilger (Ed.), McGraw-Hill International Book Co., New York (1989).

[27] A.S. Dukhin, S.S. Dukhin. Aperiodic capillary electrophoresis method using an alternating current electric field for separation of macromolecules. *Electrophoresis*, **26**, 2149 (2005).